



Numerical analysis and experimental investigation in the machining of AISI 316 steel

A K PARIDA*, P V RAO and S GHOSH

Department of Mechanical Engineering, Indian Institute of Technology Delhi, New Delhi 110 016, India
e-mail: asitzone4u@mech.iitd.ac.in

MS received 21 September 2018; revised 17 September 2019; accepted 12 November 2019; published online 20 December 2019

Abstract. High corrosion resistance and mechanical properties of AISI 316 stainless steel make its wide application in the nuclear power station and structural components in chemical industries. On the contrary, low thermal conductivity and high strain rate create problems during the machining of AISI 316, resulting in high cutting force and tool wear. Hence, this study investigates the thermal and mechanical behavior of AISI 316 steel during turning using a carbide tool. It is carried out in two stages: Finite element modeling (FEM) and experimental work. In the first stage, FEM is simulated using DEFORM software to study cutting forces, tool temperature, and chip morphology at different cutting speeds and feed rates. The results show that cutting speed and feed rate significantly affect the cutting force, thrust force and chip morphology. The chip morphology characteristics such as the degree of segmentation and serration frequency are studied. In the second stage, experimental trials are performed using the same input parameters to validate the simulated results. Results show a 10% error between simulated and experimental findings.

Keywords. Stainless steel; DEFORM; cutting force; simulation; FEM.

1. Introduction

Stainless steels like AISI 316 are widely used in biomedical equipment, automobiles, and petrochemical industries due to excellent mechanical properties [1]. The presence of (12–25) wt% of chromium in AISI 316 makes its high corrosion resistance. However, machining of AISI 316 by the conventional way is difficult due to high work hardening and abrasive behavior properties [2, 3]. Conventional coolants are used to overcome the above phenomena; however due to harmful effects to machinists, environment and disposal problem abandoning of its application. To reduce the cutting temperature at the cutting zone, researches have used different techniques and hence enhance the machining performance.

Ozbek *et al* [4] investigated the tool wear mechanism in turning of AISI 316 steel using Cyro-treated tungsten carbide inserts. They conclude that the use of a cryo-treated tool increases the hardness 5.4% than that of the untreated tool, which reduces notch wear at low speed; flank and crater wear at medium or high cutting speed. Jerold and Kumar [5] used carbon dioxide cooling as cryogen in turning AISI 316 steel, resulting in enhancement of tool life, surface finish. It is observed that the surface finish increased by 4–52% and a reduction of 35% cutting temperature. Manimaran *et al* [6] studied the machining of

AISI 316 steel at three cutting conditions, i.e., dry, wet and cryogenic cooling and concluding that application of liquid nitrogen reduces 59% and 32% surface roughness; reduction of 37% and 13% in grinding force than the dry and wet grinding conditions. Cicek *et al* [7] drill AISI 316 stainless steel using cryogenically treated high-speed steel. The enhancement in machinability is formulated by a reduction in surface roughness, thrust force, and hole quality, which is verified by the transformation of retained austenite to martensite.

Though the above use of cryogenic in metal cutting operation is significantly improving the machinability; however, the economic and cost consideration is not quite popular among machining industries. Another approach to enhance the machinability is the application of high-pressure coolant, which can penetrate the coolant in the contact region of chip-tool and tool-workpiece; hence reduction of tool wear [8, 9]. Naves *et al.* [10] investigate the wear mechanism in turning of AISI 316 steel by applying cutting fluids at high pressure and concentrations. The reduction in chip-tool contact length and tool wear is observed at high-pressure coolant conditions than the dry and conventional wet conditions. The use of conventional and low-pressure cooling is not effective in reducing thermal and chip tool interface temperature in metal operation reported by Kaminski and Alvelid [11]. In their work, they used ultra-pressure in the range of 40–200 MPa; resulting reduction of 40–50% of edge temperature. Ozcelik *et al* [12] compared

*For correspondence

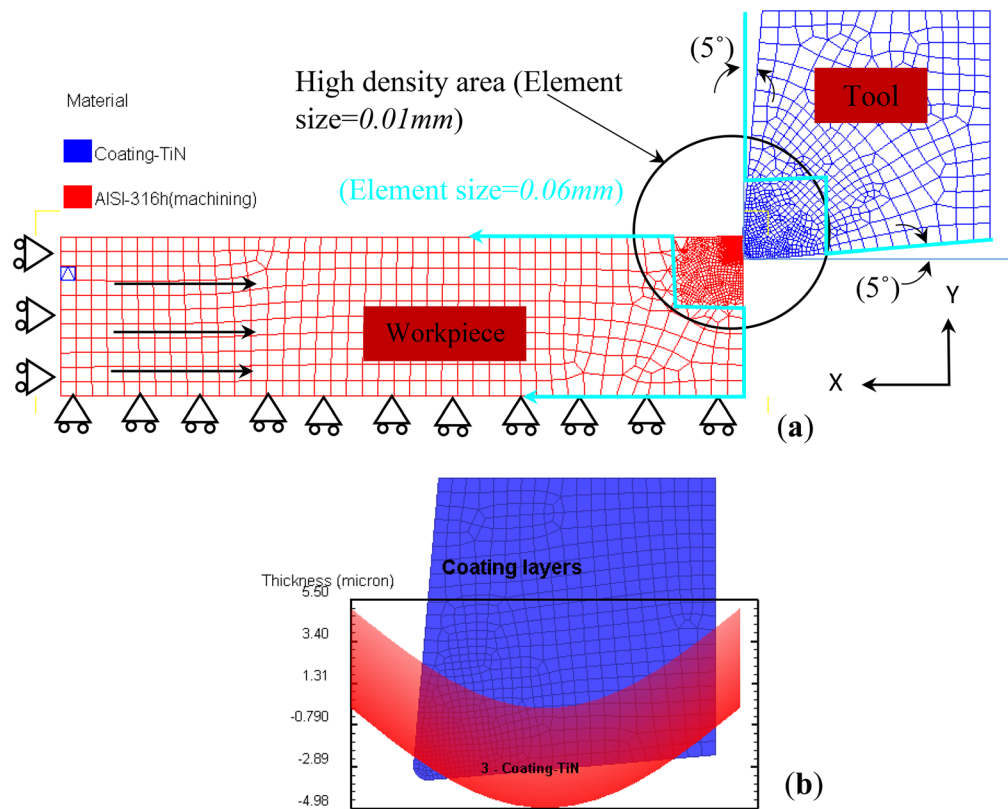


Figure 1. (a) Meshing of the cutting tool and workpiece and boundary conditions. (b) TiN coating of 5 μm on the tool.

the machinability of AISI 316 steel by varying feed rates for dry and wet milling operation. The negative influence of wet milling was observed, resulting in catastrophic failure of the cutting tool. Miromohammadsadeghi and Amirabadi [13] observed the reduction in cutting force and surface roughness in finish turning of AISI 304 using high jet pressure coolant.

From the above literature, it is revealed that the machining of AISI 316 is time and cost consuming. It is important to study the thermo-mechanical behavior of AISI 316 during the machining process by varying cutting parameters, which give higher efficiency and quality without wasting money. Numerical based finite element method is widely used in all manufacturing processes nowadays. FEM can predict the mechanical and thermal behavior of materials and tools without experimenting, hence saves cost [14]. It can also predict the responses like stress, strain, and temperature which are difficult to evaluate during experimental analysis. Different investigations of the turning of AISI 316 have already been conducted by several researchers and practitioners.

Maranhao and Davim [15] validated the cutting force, the coefficient of friction generated during machining of AISI 316 using AdvantEdge software. It concludes that the friction coefficient has a great influence on the material flow stress. Umbrello [16] presented the impacts of five unique Johnson–Cook’s constants on cutting powers, chip

morphology, and temperature using DEFORM software for the same material. It is found that the responses are significantly influenced by material constants. Nasr *et al* [17] utilized different tool edges to analyse the residual stress variation on machining of AISI 316, proposing Arbitrary Lagrangian-Eulerian (ALE) model to predict the residual stress and finally remarking that tool edge radius has a significant effect on residual stress. Bonnet *et al* [18] design a tribometer for friction model to calculate the chip-tool (AISI 316) interface where sliding velocity is more dominant for friction coefficient as compared to pressure. Naves *et al* [10] observed that high pressure cutting fluid improves tool life, and reduces cutting force while comparing the effect of lubrication on tool wear, cutting force in wet machining of AISI 316 steel with dry machining.

In the context of a 2D modeling of the orthogonal section, very few investigations have been carried out in order to determine the effect of the numerical parameters on the results of the simulation. The knowledge of the effect of certain parameters of the numerical model on the reliability of simulations presents the main purpose of this chapter. 2D model of orthogonal machining of titanium alloy Ti-6Al-4V at cutting conditions is used to determine the effect of the mesh elements (of different sizes and topologies) and numerical formulations on the results of the simulations.

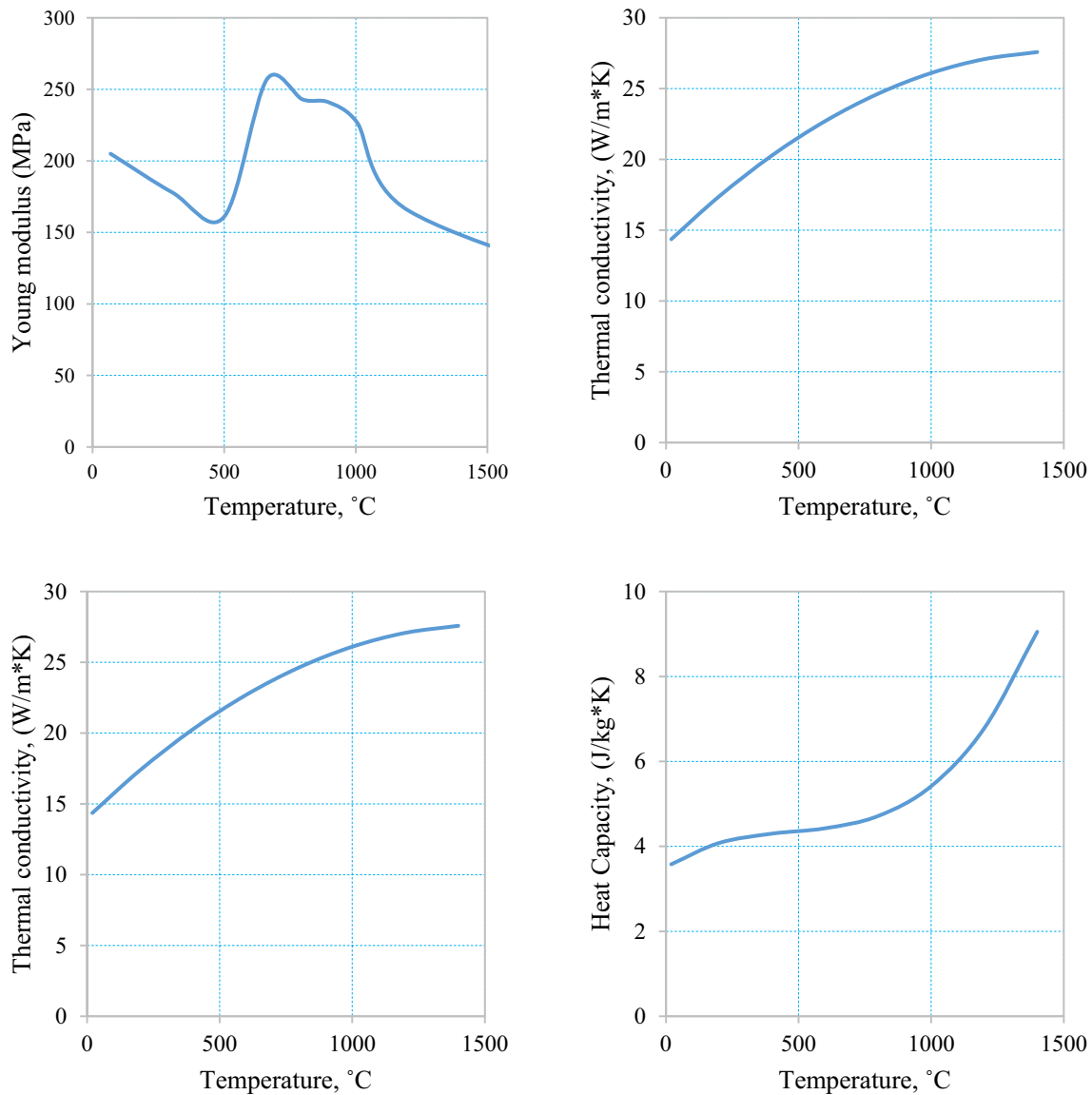


Figure 2. Graphs of mechanical and thermal properties of AISI 316 steel function of temperature.

Table 1. Chemical composition AISI 316 stainless steel (weight %).

C	Si	Mn	Ni	Cr	Mo	P	N	Co	Fe
0.010	0.630	1.280	11.140	16.74	2.020	0.020	0.030	0.240	Balance

A lot of works have already been done by the researchers on the area of machining of AISI 316 steel. However, the effect of cutting speed and feed rate on forces, chip morphology, and tool temperature has not been revealed yet by using FEM, creating a research gap. The machining process is a non-linear process due to the high plastic deformation of the metal. The advantage of FEM is the observation of different parameters such as stress, strain, and temperature

that are difficult to obtain through direct experiments. Apart from that, FEM also provides cost and time saving through the interface of simulation. Hence, the present investigation aims to study the effect of cutting speed and feed rate on cutting force and chip morphology characteristics in turning of AISI 316 using DEFORM. To validate the results of simulations, experimental works have been carried out with the same input conditions.

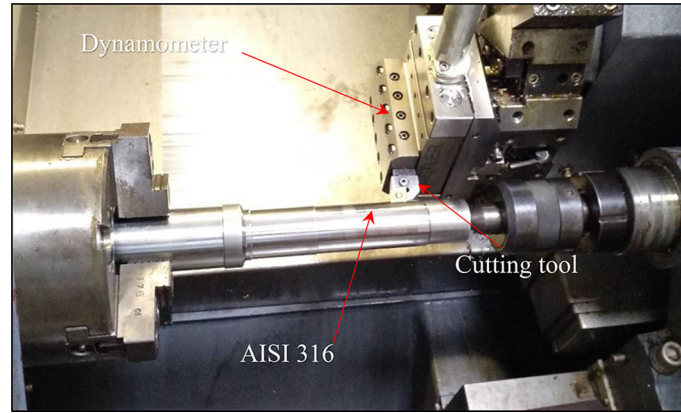


Figure 3. Experimental set-up.

2. Simulation and experimental procedure

2.1 Simulation cutting process

DEFORM 2D is a finite element code based on updated Lagrangian formulation designed to analyze forming, machining, and other thermal treatment process [19]. It provides a relevant understanding of chip formation mechanism, heat generation in cutting areas, tool-chip frictional characteristics and integrity of machined surfaces. It provides a good understanding of the effect of some physical parameters on the temperatures and stress distribution both in the tool and the workpiece. The geometry in this case workpiece is defined as a rectangle of 4 mm in length and 1.7 mm in height. The length is sufficient to allow a steady state machining process that allows the stabilization of the main magnitudes of the machining. The height ensures that the boundary conditions imposed on the base of the part will not affect the cutting area. A minimum element of size 0.01 mm is introduced at the cutting area where temperature, stress, and strain are the focus area for better accuracy of simulation results, whereas 0.06 mm element size is introduced rest area of the workpiece and cutting tool as shown in figure 1. The workpiece meshes with 30,000 elements and cutting tool meshed with 15,000 elements. The workpiece is moved in the x -direction and constraint in the y -direction, whereas the tool is fixed in both directions. The thermal and mechanical properties of the workpiece at the function of temperature are shown in figure 2. The Johnson–Cook material model is utilized for AISI 316 workpiece material and can be expressed in Eq. (1).

$$\sigma = (A + B\varepsilon^n) \left(1 + C \ln \left(\frac{\dot{\varepsilon}}{\dot{\varepsilon}_0} \right) \right) \left(1 - \left(\frac{T - T_{room}}{T_{melt} - T_{room}} \right)^m \right) \quad (1)$$

where σ is the flow stress, ε = equivalent plastic strain, $\dot{\varepsilon}$ = strain rate, $\dot{\varepsilon}_0$ = reference strain rate, T = temperature, T_{room} = room temperature, T_{melt} = melting temperature.

The Johnson–Cook material constants (A , B , C , n , and m) are taken from work [16]. During machining, severe plastic deformation occurs due to friction interaction of tool and workpiece. Therefore, the management of contact is an essential step to succeed in the elaboration of the finite element cutting model, and coulomb's friction is considered as expressed in Eq. (2).

$$\tau = \mu \sigma_p \quad (2)$$

where τ = frictional stress, Coefficient of friction, $\mu = 0.8$ [15] and σ_p = Interface pressure

Cockroft and Latham's fracture criteria are utilized to predict the effect of tensile stress on-chip segmentation as expressed in Eq. (3) [16].

$$\int_0^{\varepsilon_f} \sigma_1 d\varepsilon = D \quad (3)$$

where ε_f is the effective strain, σ_1 is the principal stress and D is a material constant.

2.2 Experimental validation

A round bar of (45 × 250 mm) AISI 316 steel is used in the experiment, and chemical composition is tabulated in table 1. The machining trials are performed in a CNC machine using a tungsten carbide insert (TiN coating) with edge radius 0.05 mm in all experiments (figure 3). Insert is mounted on left-hand tool holders with rake angle + 5°, and 5° clearance angle. In each experiment, a new cutting edge is employed for adequate comparison of cutting forces, tool wear and surface roughness. All experiments are conducted with ranges of cutting speeds (60–160 m/min) feed rates (0.1–0.13 mm/rev) and 1 mm width of cut. No cutting fluid is used in the present work. The selected cutting ranges are taken based on the literature [16]. The forces are recorded with the help of a piezoelectric

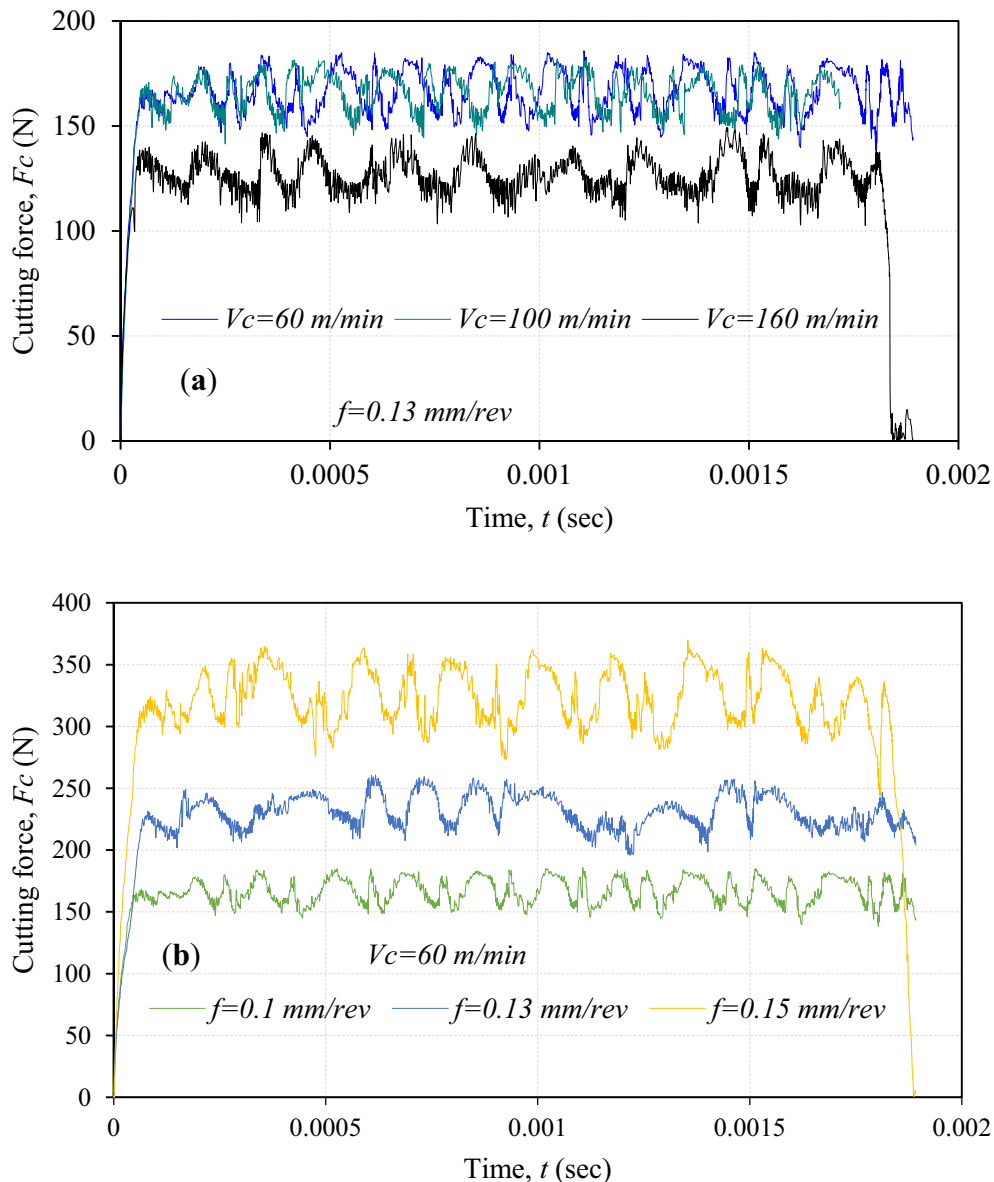


Figure 4. Simulated cutting forces at (a) different cutting speeds and (b) different feed rates.

dynamometer, and for chip morphology an optical microscope is used.

3. Results and discussion

The simulations are performed at different cutting conditions (cutting speed and feed rate). Cutting forces, temperature, stress, strain and chip morphology are predicted; and discussed in the below sections.

3.1 Cutting force, stress and temperature

The simulated cutting forces are extracted at steady-state conditions. Figure 4a shows simulated cutting force

generated at different cutting speeds and feed of 0.13 mm/rev. Fluctuating cutting forces are generated in all ranges of cutting speeds. However, cutting forces decrease with the increase in cutting speed. This could be at higher cutting speed; thermal softening phenomena occur than that of low cutting speed. This can be verified as in figure 5a; the rise in cutting zone temperature at higher cutting speed compared to low cutting speed. The thermal softening behavior of the workpiece at higher cutting speed, i.e. 160 m/min reduces the flow stress to 1030 MPa (figure 5b) from 1670 MPa at 60 m/min (figure 5c). The reduction in flow stress of workpiece does not only reduce the cutting force on the tool; but also tool temperature. Similarly, the effect of feed rates on cutting forces is also predicted at a constant speed of 60 m/min as shown in figure 4b.

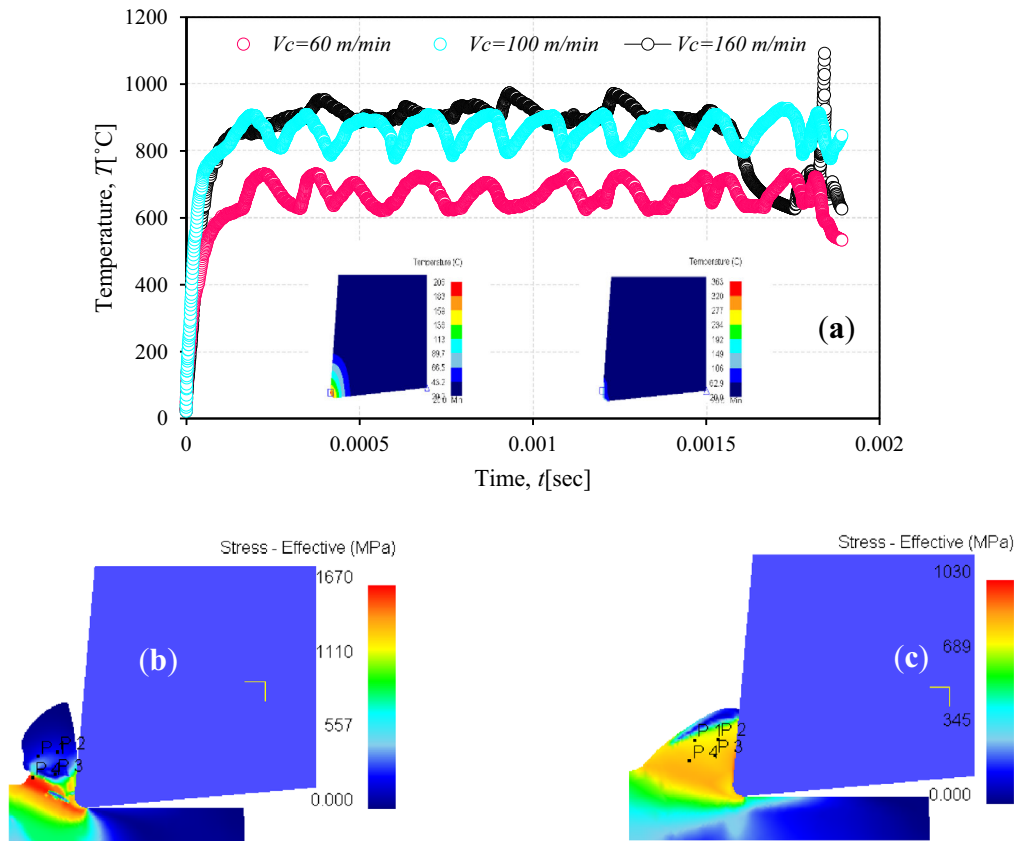


Figure 5. (a) Simulated temperature distribution generated at $f = 0.1$ mm/rev and different cutting speeds, (b) stress at $V_c = 60$ m/min and (c) stress at $V_c = 160$ m/min.

Fluctuating type of forces is observed in all ranges of feed rate; however, the trend of fluctuating decreases with the rise of feed rate. It is also observed that the cutting forces are increased with the rise of feed rate. This could be at the higher feed, more chatter or vibration as compared to low feed rate. For low test cutting speed (60 and 100 m/min) and with the feed rate of 0.13 mm/rev, the results are scattered because of the strong vibrations generated by the irregular flow of the material at low machining speeds.

The changes in temperature and effective stress in the primary cutting zone for low and high cutting speed can be reported by point tracking method. So, four points are selected on the undeformed chip thickness before it reaches the primary shear zone. At primary shear zone, a higher increase of stress, strain, strain rate, and temperature is observed. The variation between simulated and experimental results is shown in figure 6. The relative error between simulated and experimental cutting force is calculated as Eq. (4).

$$\text{Relative error} = \frac{|\text{Experimental result} - \text{Simulated result}|}{\text{Experimental result}} \times 100 \quad (4)$$

The deviation of cutting force between experimental and simulated results may be due to material properties data incorporated in DEFORM software. In all cutting speed cases, the simulated cutting forces are underestimated compared to experimental forces.

3.2 Chip morphology characteristics

In material removal procedures all have one thing in common: the formation of the chip. So, after each cutting condition, the chips are collected and kept in plastic bags. The macroscopic aspect of chips gave the general idea of chips and found that chips are helical, spiral, and long. However, to analyse the chip at the microscopic level the chip is studied under the optical microscope after polishing with different grades of emery papers. Figure 7 gives an idea of the morphology of resulting simulation chip as well as damage in the chip at higher cutting speed during machining of AISI 316. The chip morphology parameters such as chip peak (H), chip valley (h) and chip segment length (L) are measured from the simulated chip segment, whereas experimental chips are studied under optical microscopy. The experimental chip morphology is fairly coherence with the simulated chip. At low cutting speed,

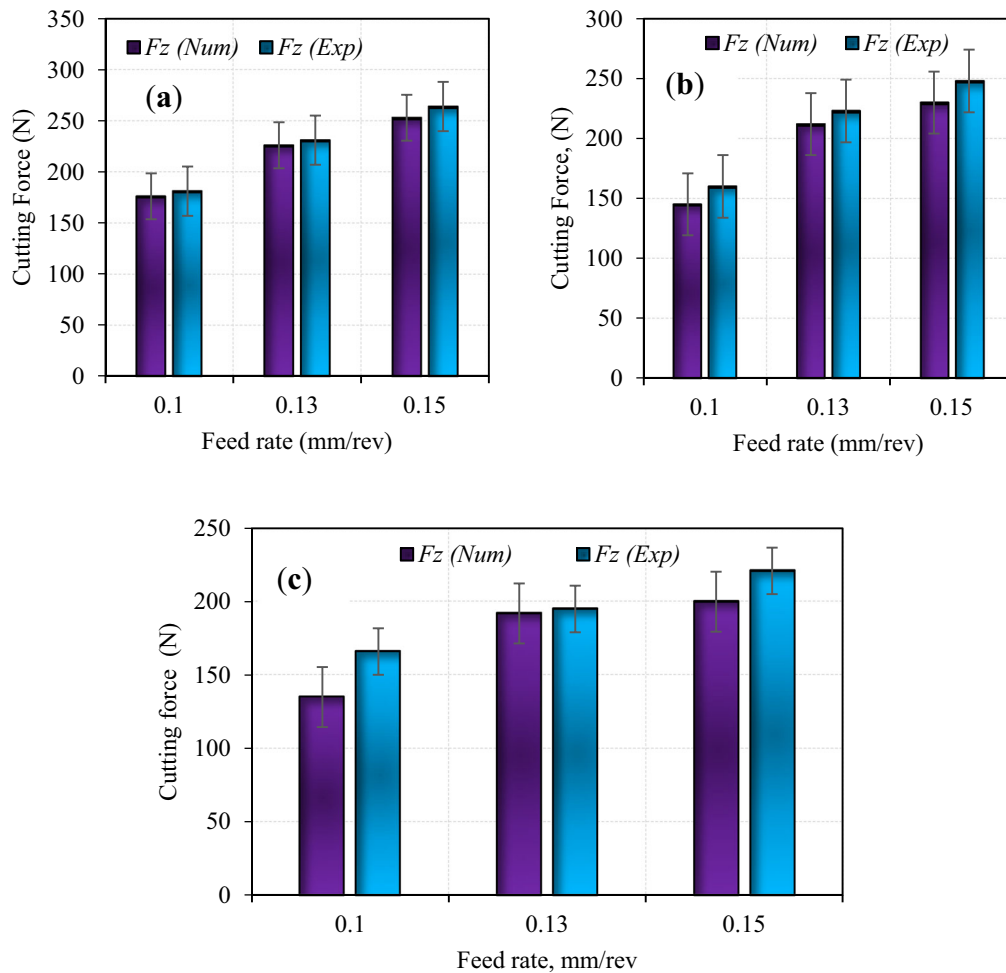


Figure 6. Variation in force at different cutting speeds (a) 60 m/min, (b) 100 m/min, (c) 160 m/min between simulated and experimental methods.

i.e., 60 m/min, the continuous chips are formed whereas, at 160 m/min, the segmented chip is noticed. This is because the distribution of temperature at the shear zone increased with the rise in cutting speed, which possibly indicates the crack. This crack goes through the primary shear zone from two side entry and out (figure 7). It is also observed that the shape of the chip segment from simulation is great coherence (periodic chip segmentation) with the experiment. Segments are separated by a band strongly damage, which bears the thermo-mechanical loading in the area before and during propagation of cracks.

To know the crack though the primary shear zone, temperature, effective stress and strain at four points are extracted though the point tracking method as shown in figure 8. Near the primary shear zone, all the responses such as temperature, effective stress and strain are increased in all points, which indicate the cracks increased from point 4 toward point 1. The maximum chip temperature increased from 764 to 882°C from cutting speed of 60 to 160 m/min. It is also observed the machined surface temperature increased with the increase of cutting speed.

Measurements of average thicknesses of chips are used to quantify the length application of the heat flux in the primary shear zone. When the chips collected after machining, only the average value of the thickness will be retained. Measurement of chip thickness changes with variation of the cutting speed and feed rate. The magnified view has been given to study the sawtooth chip at different cutting speeds for simulated and experimental chip segments as shown in figure 9.

The degree of segmentation (D_G) at different cutting speeds and feed rates is shown in figure 10 and can be calculated using Eq. (5) [20].

$$D_G = \frac{H - h}{H} \tag{5}$$

where H and h represent the peak and valley of chip respectively. The experimental degree of segmentation value increases with the increase of cutting speed and a positive correlation is observed with the experimental values. It is observed that the degree of segmentation increases linearly with the rise of feed rate and cutting speed. Close

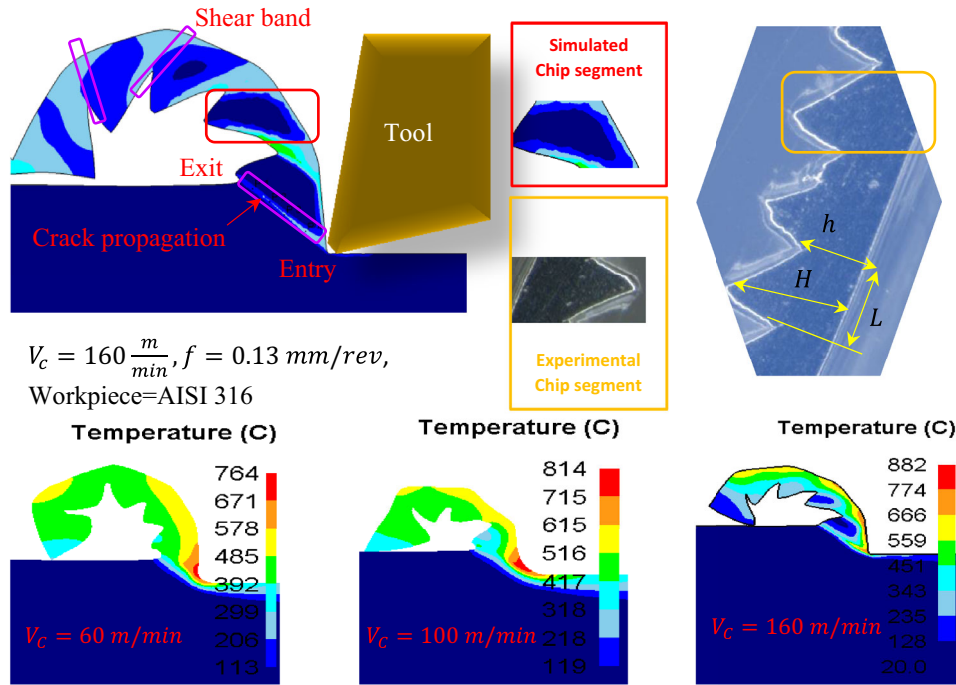


Figure 7. Measurement of chip morphology parameters and chip temperature at different cutting speeds.

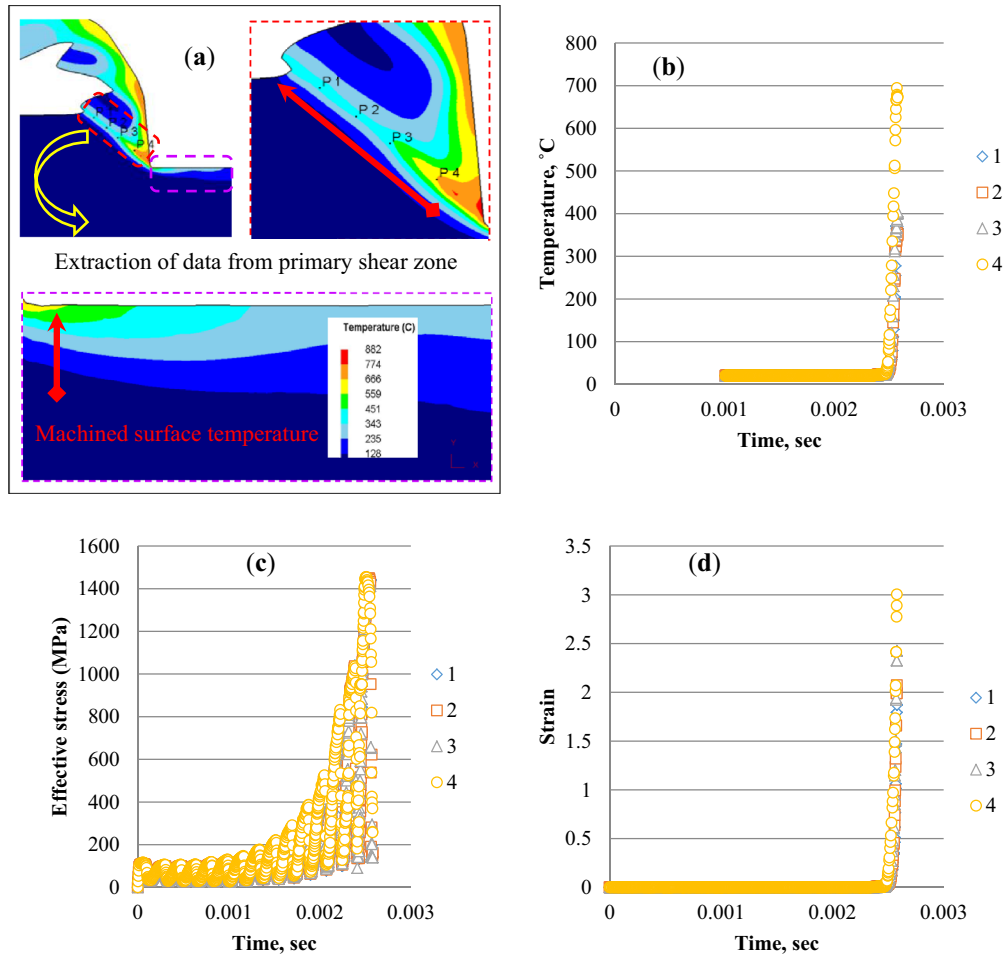


Figure 8. Extraction of parameters from shear zone (a), Temperature (b), Effective stress,(c) and Strain (d).

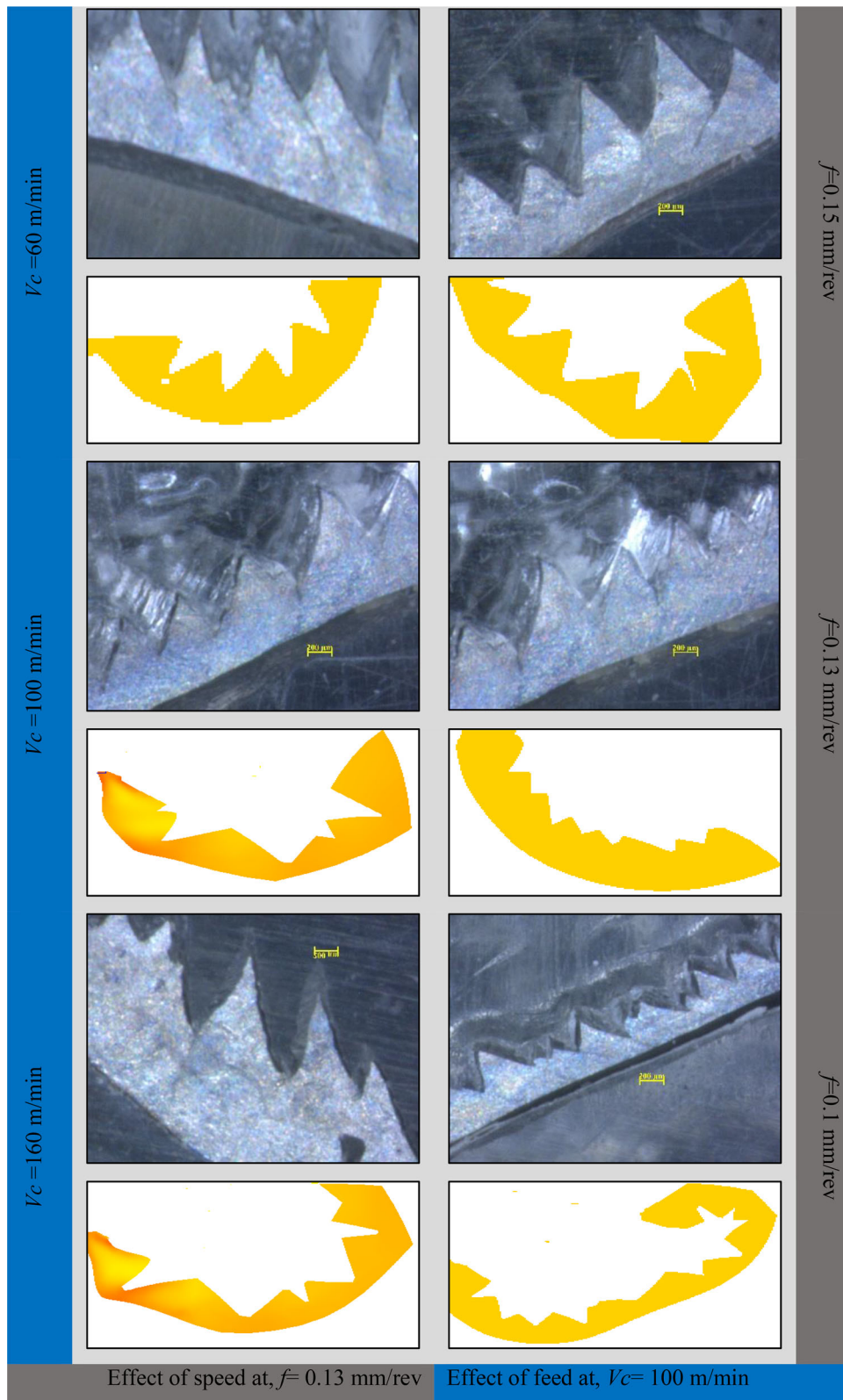


Figure 9. Effect of cutting speed and feed rate on chip morphology.

agreement between the simulated and experimental degree of segmentation is observed at a cutting speed of 100 m/

min; whereas near about 10% error is observed at a cutting speed of 60 and 160 m/min respectively.

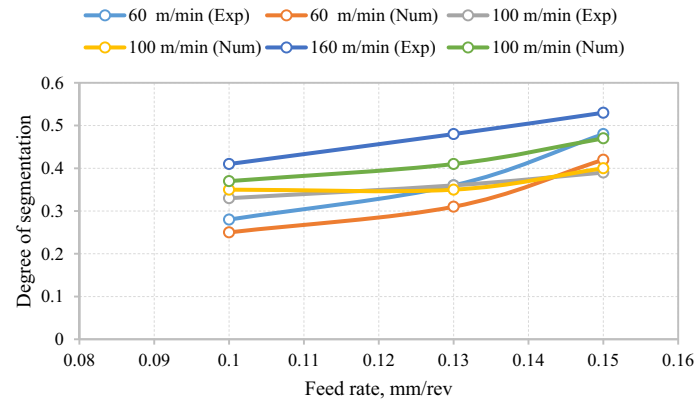


Figure 10. Comparison of the simulated and experimental degree of segmentation at different cutting speed and feed rate.

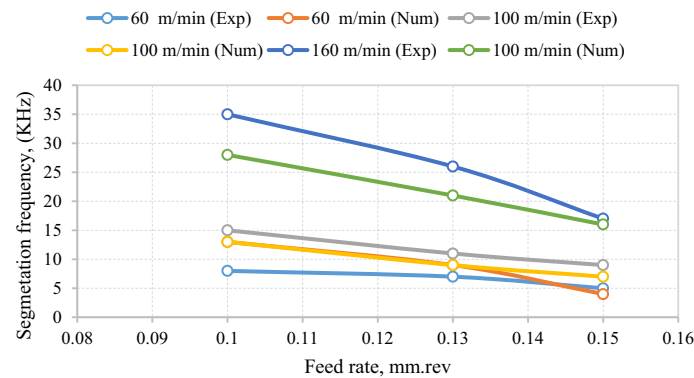


Figure 11. Comparison of simulated and experimental segmentation frequency at different cutting conditions.

Similarly, the effect of cutting speed and feed rate on segmentation frequency (f_c) is shown in figure 11 and can be calculated by using Eq. (6) [21].

$$f_c = \frac{V_c}{L} \tag{6}$$

where L is the average of the crack-tooth spacing chip segment.

The serration frequency is low at a high feed rate and cutting speed; however, its value is high at low cutting speed and feed rate respectively. More serration in the chips with an increase of feed rate leads to impact stress on the tooltip. Thus machining of AISI 316 at higher feed rate leads to an increase in cutting force. At higher cutting speed, there is a large discrepancy between simulated and experimental serration frequency.

4. Conclusions

In this research work, finite element modeling is utilized to simulate the machining of AISI 316 using DEFORM software. The responses such as cutting force, stress,

temperature, and chip morphology parameters in turning of AISI 316 are simulated with a variation of cutting speed and feed rate. Experiments are performed with the same input parameters to validate the simulation results. From the analysis, the following conclusions can be made:

1. The variation in cutting forces in machining of AISI 316 shows reduction tendency when cutting parameters are changes for both experimental and simulation conditions. At lower cutting speed it is observed that the chip formation is continuous whereas by increasing the cutting speed up to 160 m/min, segmented type of chip is noticed. Chip segmentation is explained as occurring when the stress generated in the shear plane is greater than the ultimate stress of the workpiece material.
2. The chip segment characteristics such as the degree of segmentation and serration frequency are affected by cutting parameters. The degree of segmentation of chip increases with the increase in cutting speed; however, serration frequency is reduced with the increase in feed rate.
3. Chip’s temperature increased with both high cutting speed and feed rate. From a practical point of view, it is required to choose conditions that allow the removal of

heat by the chip in order to save the cutting tools from thermal damage.

4. The simulated forces are validated with the experimental findings to show a 10% error in between. Thus a more feasible and reliable simulation may have been established by varying friction value, mesh size and damage factor for better results.
5. In the future, 3D model simulation can be utilized for a better understanding of multi-physical phenomena in machining of AISI 316.

References

- [1] Saoubi R M, Outeiro J C, Changeux B, Lebrun J L and Mora A 1999 Residual stress analysis in orthogonal machining of standard and desulfurized AISI 316L steels. *Journal of Material Processing Technology* 96: 225–233
- [2] Varghese V, Ramesh M R and Chakradhar D 2018 Experimental investigation and optimization of machining parameters for sustainable machining. *Mater. Manuf. Process* 00: 1–11. <https://doi.org/10.1080/10426914.2018.1476760>
- [3] Ranganathan S, Senthilvelan T and Sriram G 2010 Evaluation of machining parameters of hot turning of stainless steel (Type 316) by applying ANN and RSM. *Mater. Manuf. Process*. 25: 1131–41. <https://doi.org/10.1080/10426914.2010.489790>
- [4] Altan N, Çiçek A, Gülesin M and Özbek O 2016 Effect of cutting conditions on wear performance of cryogenically treated tungsten carbide inserts in dry turning of stainless steel. *Tribology Int.* 94: 223–33. <https://doi.org/10.1016/j.triboint.2015.08.024>
- [5] Jerold B D and Kumar M P 2012 Machining of AISI 316 stainless steel under carbon-Di-Oxide cooling. *Mater. Manuf. Process*. 1059–1065. <https://doi.org/10.1080/10426914.2011.654153>
- [6] Manimaran G, Pradeep Kumar M and Venkatasamy R 2014 Influence of cryogenic cooling on surface grinding of stainless steel 316. *Cryogenics* 59: 76–83. <https://doi.org/10.1016/j.cryogenics.2013.11.005>
- [7] Cic A and Uygur I 2015 Machinability of AISI 316 austenitic stainless steel with cryogenically treated M35 high-speed steel twist drills. 134: 1–6. <https://doi.org/10.1115/1.4007620>
- [8] Katoh T, Ohmori S, Maeda T, Kakumitsu T and Okuda K 2015 Effect of High-pressure coolant supply on chip-breaking and tool wear in the machining of stainless steel; 657: 226–230. <https://doi.org/10.4028/www.scientific.net/kem.656-657.226>
- [9] Mia M and Dhar N R 2018 Effects of duplex jets high-pressure coolant on machining temperature and machinability of Ti-6Al-4V superalloy. *J. Mater. Process. Technol.* 252: 688–96. <https://doi.org/10.1016/j.jmatprotec.2017.10.040>
- [10] Naves V T G, Da Silva M B and Da Silva F J 2013 Evaluation of the effect of application of cutting fluid at high pressure on tool wear during turning operation of AISI 316 austenitic stainless steel. *Wear* 302: 1201–1208. <https://doi.org/10.1016/j.wear.2013.03.016>
- [11] Kaminski J and Alvelid B 2000 Temperature reduction in the cutting zone in water-jet assisted turning. *Journal of Material Processing Technology* 106: 68–73
- [12] Ozcelik B, Kuram E, Simsek B T, Ozcelik B, Kuram E and Simsek B T 2011 Comparison of dry and wet end milling of AISI 316 stainless steel. *Mater. Manuf. Process*. 6914. <https://doi.org/10.1080/10426914.2010.515645>
- [13] Amirabadi H 2018 High-pressure jet-assisted turning of AISI 304: Experimental and multi-objective optimization approach. In: *Proceedings of the Institution of Mechanical Engineers, Part E: Journal of Process Mechanical Engineering*. 232: 734–750. <https://doi.org/10.1177/0954408917738488>
- [14] Davim J P, Maranhão C, Jackson M J, Cabral G and Grácio J 2008 FEM analysis in high-speed machining of aluminum alloy (Al7075-0) using polycrystalline diamond (PCD) and cemented carbide (K10) cutting tools. *Int. J. Adv. Manuf. Technol.* 39: 1093–100. <https://doi.org/10.1007/s00170-007-1299-y>
- [15] Maranhão C and Paulo Davim J 2010 Finite element modeling of machining of AISI 316 steel: Numerical simulation and experimental validation. *Simul. Model. Pract. Theory*; 18: 139–56. <https://doi.org/10.1016/j.simpat.2009.10.001>
- [16] Umbrello D, M'Saoubi R and Outeiro J C 2007 The influence of Johnson-Cook material constants on finite element simulation of machining of AISI 316L steel. *Int. J. Mach. Tools Manuf.* 47: 462–70. <https://doi.org/10.1016/j.ijmactools.2006.06.006>
- [17] Nasr M N A, Ng E G and Elbestawi M A 2007 Modelling the effects of the tool-edge radius on residual stresses when orthogonal cutting AISI 316L. *Int. J. Mach. Tools Manuf.* 47: 401–11. <https://doi.org/10.1016/j.ijmactools.2006.03.004>
- [18] Bonnet C, Valiorgue F, Rech J, Bergheau J M, Gilles P and Claudin C 2008 Development of a friction modeling method in dry cutting of AISI 316L austenitic stainless steels. *International Journal of Material Forming* 1: 1211–1214. <https://doi.org/10.1007/s12289-008-0159-0>
- [19] DEFORM 3D Version 11.0, User Manual. SFTC, Columbus, Ohio State. 2016
- [20] Müller C, Blümke R, Mu C and Blu R 2017 Influence of heat treatment and cutting speed on-chip segmentation of age hardenable aluminum alloy. *Materials Science and Technology* 17: 651–654.
- [21] Kishawy H A and Hosseini A 2019 *Machining difficult-to-cut materials*. Springer, Canada